https://doi.org/10.5194/egusphere-2026-3590
Preprint. Discussion started: 30 June 2026

Revisiting overflow metabolism and its impact on soil carbon cycling

José M. Murúa Royo[1], Brittni L. Bertolet[1,3], Luciana Chavez Rodriguez[1,4], Jeth Walkup[1], Steven D. Allison[1,2]

[1]Department of Ecology and Evolutionary Biology, University of California, Irvine, Irvine, 92697, USA
[2]Department of Earth System Science, University of California, Irvine, Irvine, 92697, USA
[3]Department of Earth and Environmental Science, Rutgers University Newark, Newark, New Jersey, USA
[4]Soil Biology Group, Wageningen University & Research, Wageningen, Gelderland, The Netherlands

Correspondence to: José M. Murúa Royo (jmuruaro@uci.edu)

Abstract. A major challenge in biogeochemistry is to reduce the uncertainty of projections made by soil carbon models. In the last two decades, carbon-use efficiency, the proportion of consumed carbon incorporated into microbial biomass, has become a central parameter to represent microbial control on carbon fluxes. For models that integrate other elements, like nitrogen, the adjustment of carbon-use efficiency in response to substrate stoichiometry has gained popularity as a mechanism to balance these fluxes, mostly due to its mathematical convenience. The reasoning behind this, is that microbes release the excess carbon as CO_2, a mechanism known as overflow respiration. This mechanism, however, causes a characteristic decrease of carbon-use efficiency when reaching nitrogen limitation. In this study we propose that the implementation of overflow respiration forces an unrealistic decrease of carbon-use efficiency for three reasons: 1) physiological mechanisms can minimize carbon excess, avoiding overflow; 2) carbon overflow has been reported in laboratory experiments mainly as dissolved organic carbon (organic acids), and not as CO_2; 3) functionally diverse microbial communities can exhibit higher-level dynamics, improving the recycling of nutrients and avoiding overflow. We use an individual-based microbial litter decomposition model to test the impact of these mechanisms on carbon-use efficiency. We found that physiological mechanisms such as flexible biomass stoichiometry can eliminate overflow, but nutrient allocation does not. When carbon overflow occurs as dissolved organic carbon, carbon-use efficiency increases under nitrogen limitation. Finally, a functionally diverse community can avoid carbon overflow, although carbon-use efficiency declines due to higher maintenance respiration. We demonstrate that the representation of overflow respiration in soil carbon models is more relevant than currently acknowledged. Redirecting carbon overflow to a dissolved organic carbon pool can lead to opposite trends in carbon losses. The soil carbon modeling community should thoroughly assess current implementations and explore more mechanistically grounded alternatives. This includes dissolved organic carbon pathways, more realistic microbial community representations, or other processes that better capture the complexity of microbial carbon use.

https://doi.org/10.5194/egusphere-2026-3590
Preprint. Discussion started: 30 June 2026

1. Introduction

Estimating carbon (C), nitrogen (N) and phosphorus (P) mineralization from soil organic matter is fundamental to predict future ecosystem responses to environmental change. Biogeochemical models are the main tool to make generalized predictions of these fluxes from local to regional scales. Over the last few decades, soil biogeochemical models have explicitly incorporated soil microbial biomass pools that mediate the decomposition of soil organic C (Allison et al., 2010; Fontaine & Barot, 2005; Schimel & Weintraub, 2003; Wieder et al., 2013). These modeling improvements have increased our predictive power of soil C projections under environmental change (Allison et al., 2010; Wieder et al., 2013). Microbial-explicit models enabled us to identify carbon-use efficiency as a key parameter determining the fate of C (Allison et al., 2010; Li et al., 2014; Tao et al., 2023; Wieder et al., 2013). However, carbon-use efficiency is a complex parameter affected by many variables (Hagerty et al., 2018; Manzoni et al., 2012).

Among the factors influencing carbon-use efficiency is the elemental imbalance that exists between soil microbial biomass (e.g., C:N ~ 8) and its growth substrate, plant litter (e.g., C:N = 10–120). Traditionally, models have assumed that soil microbes increase C excretion to eliminate the excess of C when growing on high C:N substrate, a mechanism referred to as 'overflow metabolism' (sensu Schimel & Weintraub, 2003). This excretion of excess C, particularly in the form of CO_2 (overflow respiration), has become widely used in soil models to balance the fluxes of C and nutrients (Abramoff et al., 2017; Allison, 2012; Averill, 2014; Bosatta & Berendse, 1984; Hadas et al., 1998; Huang et al., 2018; Kaiser et al., 2014; Kersebaum & Richter, 1994; Kyker-Snowman et al., 2020; Manzoni et al., 2021; Moorhead et al., 2012; Raynaud et al., 2006; Schimel & Weintraub, 2003; Shaffer et al., 2015; Sistla et al., 2014; Wutzler et al., 2017). Imposing this mechanism leads to a decrease in carbon-use efficiency upon reaching nutrient limitation. Consequently, many soil models estimate high rates of soil respiration (Manzoni & Porporato, 2009; Spohn, 2015) and lower C sequestration for high C:N litter. Despite its popularity, overflow respiration has faced little empirical validation.

Overflow respiration was originally presented by Schimel and Weintraub (2003) as a balancing mechanism for C and N fluxes. Beyond its mathematical convenience, the justification for this mechanism comes from the literature in microbiology, where the term 'overflow metabolism' was originally coined (Tempest & Neijssel, 1992). This term describes the excretion of organic acids, such as acetate, when microbes face specific growth-limiting conditions (e.g., NH4 limitation). The vast majority of these reports describe C overflow in the form of organic acids as opposed to CO_2 (Chowdhury et al., 2025; Neijssel & Tempest, 1975). This simple difference can have relevant implications for the fate of C in the soil system. Organic acids can be used as a C source by other microbes, which can increase the residence time of C in soil and potentially be stabilized.

https://doi.org/10.5194/egusphere-2026-3590
Preprint. Discussion started: 30 June 2026

Other physiological mechanisms may also decrease elemental imbalance and can have further consequences for the fate of C and nutrients in soil. For instance, extracellular enzyme allocation (Moorhead et al., 2012), uptake allocation (Logan et al., 2004), and flexible biomass stoichiometry (Allison, 2012; Manzoni et al., 2021) can contribute to reducing elemental imbalances. These mechanisms have been rarely included in soil models (Manzoni & Porporato, 2009) but some studies have highlighted their implications for decomposition, nutrient mineralization, and C stabilization in soils (Kaiser et al., 2014; Manzoni et al., 2021). For example, if microbial decomposers use enzyme and uptake allocation to solve their elemental imbalance, limiting elements may be depleted faster than abundant ones. Consequently, the decomposition of organic matter would slow down since many C compounds would be left behind (Boberg et al., 2008; Manzoni et al., 2021). Moreover, the sequential nature of these mechanisms implies that solving imbalances before excretion could potentially avoid the occurrence of overflow. Therefore, carbon-use efficiency would be higher than expected by overflow respiration which could potentially lead to more biomass and necromass production, and consequently, more C sequestration in soils receiving high C:N litter.

Apart from physiological mechanisms operating at the level of organisms, elemental imbalances can also be reduced by population dynamics. More specifically, labor division between different functional groups can lead to the regulation of nutrient uptake into the community. Folse & Allison (2012), found in simulation experiments that for communities where labor was divided among C, N, and P depolymerization, specialists not only were able to maintain coexistence, but population dynamics acted to regulate enzyme production. The result was an overall reduction in substrate depolymerization compared to communities without division of labor. Later, Kaiser et al. (2014) found that communities with plant and necromass specialists increased the turnover rate of N relative to C. This increased N recycling capacity relieved the elemental imbalance with litter, effectively decoupling litter C:N from decay rates. Furthermore, the authors reported a convergence in community carbon-use efficiency at around 0.32 independent of initial litter C:N. Therefore, complex communities with low functional redundancy among taxa can regulate the use of elements at the community level.

In this study we consider different mechanisms for coping with elemental imbalance and quantify their impact on soil C dynamics. We propose that the reduction of carbon-use efficiency for C:N litter caused by an imposed mechanism of overflow respiration is unrealistic. We predict that carbon-use efficiency can remain at high values in these conditions via three non-mutually exclusive mechanisms: 1) physiological acclimation mechanisms that solve the elemental imbalance before overflow happens; 2) the occurrence of C overflow as dissolved organic C (DOC) instead of CO_2; and 3) a functionally diverse community with division of labor that enhances the recycling of the limiting element, further reducing the elemental imbalance. To assess the impact of these mechanisms on the fate of C and nutrients, we performed an *in silico* experiment using a microbial-based model of plant litter decomposition, quantifying key processes to estimate C and nutrient balance. We implement different simulation scenarios based on the nature of overflow (CO_2 or DOC), activation of different physiological mechanisms, and the level of functional redundancy in the microbial community.

https://doi.org/10.5194/egusphere-2026-3590
Preprint. Discussion started: 30 June 2026

2. Methods

2.1 Model description

Simulations were performed with the Decomposition Model of Enzymatic Traits (DEMENT; Allison, 2012). Figure 1 depicts the individual-based nature of the model. DEMENT was originally designed to link soil microbial functional diversity with ecosystem function (e.g., decomposition, nutrient mineralization, respiration, etc.). The model focuses on effect traits (i.e., traits that directly impact ecosystem function) like extracellular enzymes and transmembrane transporters, as well as response traits that mediate the population dynamics under environmental factors like soil temperature and moisture. This design effectively links environmental change with changes in ecosystem function and has successfully been used to simulate responses to climate warming (Allison, 2014), drought (Allison & Goulden, 2017; Wang & Allison, 2021), and microbiome transplantation across climatic gradients (Wang & Allison, 2022).

We used DEMENT as a simulation platform to test our hypotheses for carbon-use efficiency. DEMENT is an ideal tool for this objective because carbon-use efficiency is not an explicit parameter. Rather, it is treated as an emergent property driven by different cellular processes like substrate assimilation efficiency, biomass-specific respiration, and overflow respiration. Furthermore, DEMENT requires mass balance of C, N, and P. Leaf litter is represented by 10 different polymers with varying content of C, N, and P (Table 1). The processes represented in simulations are depicted in Fig. 2. We only formalize processes relevant for microbial growth mass balance. For a complete description of the model, refer to Allison (2012), Allison (2014), and Allison & Goulden (2017). We also describe the main model processes in the appendix. Environmental modulation of the processes (i.e., effects of temperature and moisture) were omitted from process descriptions since we held environmental variables constant (temperature = 5˚C, water potential = -0.2) and focused on changes in leaf litter C:N.

https://doi.org/10.5194/egusphere-2026-3590
Preprint. Discussion started: 30 June 2026

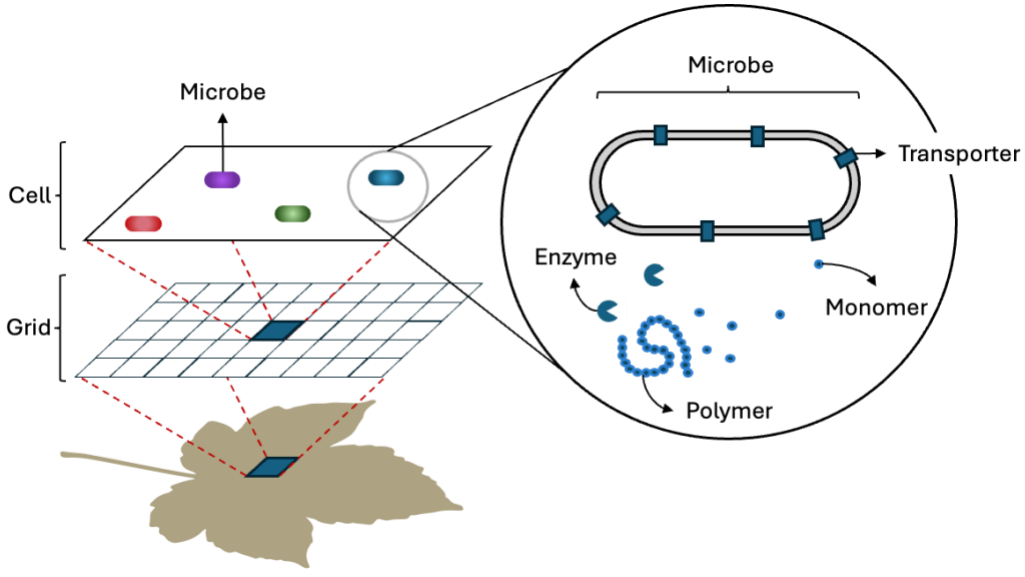

Figure 1. Structure of DEMENT. Leaf litter is represented as a two-dimensional grid. By mass, the entire grid represents 1 cm2 of leaf litter. Processes are computed grid-wise, where several microbes can co-exist in a single grid box and interact. Different types of microbes are represented by traits like extracellular enzymes and transmembrane transporters. Extracellular enzymes mediate the degradation of leaf litter polymers into monomers that can be taken up by microbes via transporters. Interactions between microbes only occur through resource use, whether it is competition or cooperation (e.g., labor division, cross-feeding).

https://doi.org/10.5194/egusphere-2026-3590
Preprint. Discussion started: 30 June 2026

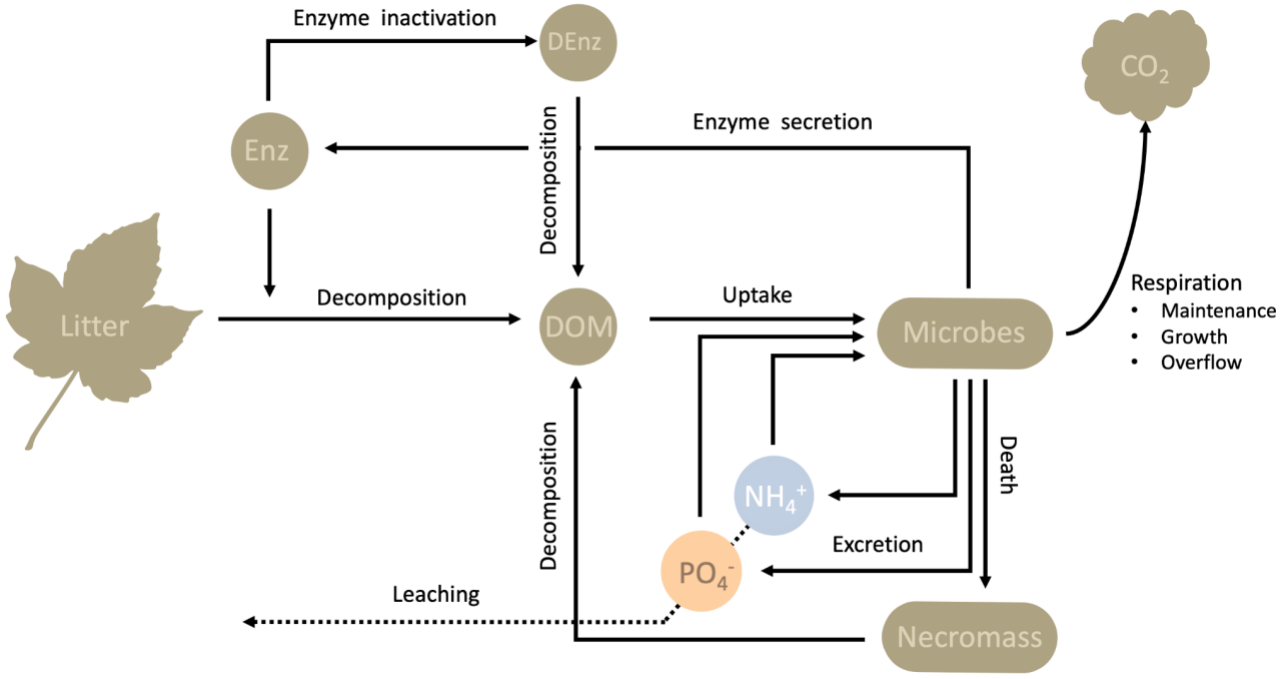

Figure 2. Pools and processes in DEMENT. Leaf litter is composed of several polymers (Table 1) which can be depolymerized by enzymes into individual monomers, represented in the diagram as dissolved organic matter (DOM). Monomers can be taken up by microbes to build new biomass or produce extracellular enzymes. Microbial growth needs to fulfill certain stoichiometric requirements (see section 2.2), therefore, elements that are in excess are disposed as CO_2 (C excess, i.e., overflow respiration), NH4 excretion (nitrogen excess), or PO4 excretion (phosphorus excess). Microbial death feeds the pool of necromass, which can be depolymerized into monomers and used as growth substrate again by microbes (necromass recycling). Extracellular enzymes have a limited "lifespan" (i.e., turnover rate), after which they become inactive and are subject to degradation and uptake.

2.2 Initialization

DEMENT permits a great diversity of enzyme (and transporter) types, allowing for promiscuity (one enzyme targeting more than one polymer) and redundancy (several enzymes targeting the same polymer). Kinetic parameters (Vmax and Km) are chosen from uniform distributions and assigned randomly to each enzyme type. For an easier causality attribution, we decided to eliminate stochastic processes in trait definition and community assembly. Consequently, our simulations use a pool of 12 enzyme types, each targeting a single polymer (i.e., no promiscuity nor redundancy), while all enzymes share the same value of Vmax and Km (supplementary material). Similarly,12 transporter types were implemented, each targeting 1 single monomer, all sharing the same kinetic parameters. All taxa possessed all transporters. The difference between taxa then was the number and type of enzymes that each taxon possessed (see section 2.3).

https://doi.org/10.5194/egusphere-2026-3590
Preprint. Discussion started: 30 June 2026

2.3 Mechanisms that solve elemental imbalance

The mechanisms that reduce elemental imbalance in DEMENT are 1) overflow respiration, and 2) flexible biomass stoichiometry, the latter being optional. Usually, nitrogen immobilization is also considered a mechanism to minimize elemental imbalance. In DEMENT, although nitrogen excretion is determined by biomass stoichiometric homeostasis, the uptake of inorganic nitrogen follows Eq. (A2) and therefore is not a function of nitrogen demand, but rather substrate concentration. Also, the current enzyme production and uptake processes lack any regulation to satisfy biomass stoichiometry homeostasis. Consequently, we develop the corresponding mechanisms of enzyme and uptake regulation for our further analyses.

2.3.3 Implementation of enzyme and uptake allocation

The original DEMENT model describes enzyme production by a constitutive term (fixed proportion of biomass) and an inducible term (fixed proportion of C uptake, see Eq. (A4)). Since enzyme production implies a cost, and an associated return that may be compromised by environmental factors (e.g., cheaters), natural selection should favor microbes that limit their enzyme secretion under conditions of low return on investment. For example, studies with S. cerevisiae describe three types of physiological responses in conditions of phosphorus starvation: 1) mobilization of internal stores of phosphate, 2) up-regulation of membrane transporters involved in phosphate uptake (Pho84), and 3) increase in production of extracellular phosphatases, like Pho5 (Thomas & O'Shea, 2005). Interestingly, at intermediate phosphorus conditions, the membrane transporter is expressed but not the phosphatase, whose expression is restricted to extreme phosphate deprivation. The cytosolic concentration of phosphate is the key regulatory factor.

To implement a generalized enzyme regulation mechanism, we assume the production of each enzyme type is regulated by the uptake of one or more elements (Table 1). The specific element regulating an enzyme depends on the stoichiometry of the targeted polymer. Consequently, cellulases are only regulated by C uptake, whereas chitinases can be regulated by C or nitrogen. In the cases where there is more than one regulating element, the current most limiting element is chosen as the regulator.

https://doi.org/10.5194/egusphere-2026-3590
Preprint. Discussion started: 30 June 2026

Table 1. Polymers in DEMENT and their elemental content

Polymer	C (%)	N (%)	P (%)	C:N	Regulating element
Cellulose	100	0	0	-	C
Hemicellulose	100	0	0	-	C
Starch	100	0	0	-	C
Chitin	83.43	16.57	0	5.04	C or N
Lignin	98.85	1.15	0	86.05	C or N
Protein1	82.45	17.55	0	4.7	C or N
Protein 2	82.45	17.55	0	4.7	C or N
Protein 3	82.45	17.55	0	4.7	C or N
Organic phosphorus 1	0	0	100	-	P
Organic phosphorus 2	0	0	100	-	P
Inactive enzymes	76.92	23.07	0	3.33	N
Necromass	Variable	Variable	Variable	Variable	N or P

We used a heuristic sigmoid function (Fig. 3) to downregulate enzyme production based on the amount of the regulating element taken up. Since the minimum quota is defined as the minimum amount of element in biomass required for survival, we used this quantity to normalize the uptake of the regulating element. The level of enzyme production repression is given by:

$$E_R = \frac{e^{a(x-b)}}{s + e^{a(x-b)}} \quad (1)$$

$$x = \frac{U_x}{B_C} \times \frac{1}{Q_{min}} \quad (2)$$

where ER is the coefficient of enzyme repression, which takes a value between 0 and 1. The variable x represents the per-capita uptake of the regulating element x normalized by its minimum quota; a = −12, b = 0.75, and s = 1 are parameters that control the shape of the sigmoid curve. The structure of the function and the values of these parameters lack any mechanistic interpretation, but they were chosen to align the resulting sigmoid curve with the expected response of gene expression (Bonachela et al., 2013; Veitia, 2003). Therefore, our approach to model enzyme regulation is not aiming for perfect stoichiometric regulation, but is a biologically reasonable approximation.

https://doi.org/10.5194/egusphere-2026-3590
Preprint. Discussion started: 30 June 2026

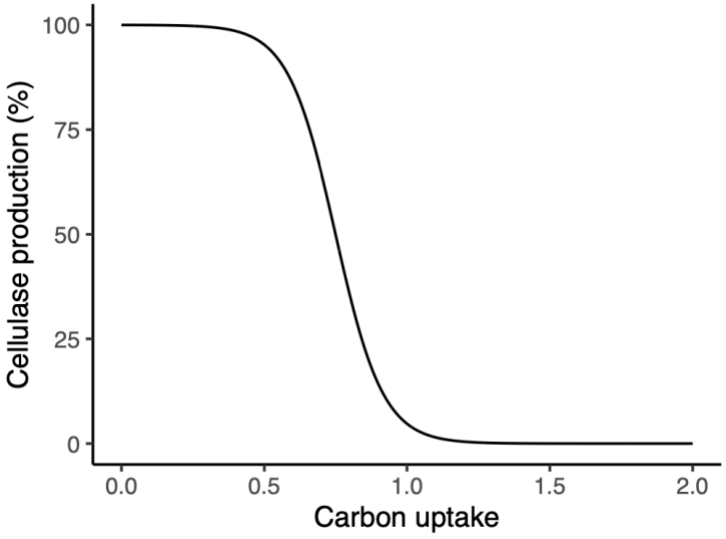

Figure 3. Sigmoid function example. The x axis is the per-capita C uptake normalized by the minimum C quota. The production of cellulase is subject to the current amount of C uptake. If uptake is close to 0, demand for C is high and cellulase is produced at maximum capacity. If uptake is close to satisfying the minimum C quota, C availability is considered sufficient for survival and cellulase production is shut down.

The updated equation for enzyme production is then:

$$E_{prod} = C_U \times E_{ind} \times E_R + B \times E_{const} \times E_R \quad (3)$$

Equation (3) shows that both the induced and constitutive enzyme production terms are being repressed. Although constitutive production should in theory remain independent, we found that repressing only the induced production leads to very small amounts of enzyme allocation patterns. In other words, the weight of the constitutive production on total production was too big. For this reason, we decided to repress both components.

We also update Eq. (A2) to incorporate uptake regulation. This decision follows the example above, where transporter abundance in the cell membrane should be reduced for transporters that target non-limiting elements.

$$Uptake = (U_A \times B \times E_R) \times (V_{max} \times \frac{S_M}{K_m + S_M}) \quad (4)$$

However, since we cannot use the level of uptake to regulate itself, we use the uptake of the previous time step.

https://doi.org/10.5194/egusphere-2026-3590
Preprint. Discussion started: 30 June 2026

2.4 Simulation setup

Our simulations consisted of a single litter cohort decomposing through a duration of 999 days. To make outputs comparable across simulations, we normalize our variables per 50% C mass loss. Therefore, a pulse duration of 999 days ensured this amount of C mass loss was achieved even for the slowest decomposing simulations. The initial litter was characterized by a specific chemistry (i.e., C:N:P content) which is dependent on the proportion of different polymers (10 first rows of Table 1). Initial litter C:N was increased from 10 to 90 by 1 unit increments for a total of 81 simulations. The total amount of initial litter C remained constant throughout the C:N range at 344.56 mg cm-2. The N content of litter was manipulated by decreasing the concentration of polymers containing N, except for lignin which remains constant throughout the range. Across the range, litter N:P was kept constant at a value of 7. For this to be possible, we assumed that the two polymers representing organic phosphorus contained no C or nitrogen (Table 1). Although this is not realistic, the assumption is reasonable considering that phosphatases act by cleaving phosphate groups from the rest of the molecule.

Next, we manipulated the presence of physiological mechanisms involved in reducing elemental imbalance (i.e., overflow, nutrient acquisition allocation, and flexible biomass stoichiometry). Overflow is the default mechanism in DEMENT and it was present in every simulation. Nutrient allocation was either absent, present as enzyme allocation only, or as both enzyme and uptake allocation (Table 2). Microbial biomass stoichiometry was kept either fixed, or allowed to vary within a tolerance range. This range was empirically informed using data of fungal strains with high stoichiometric flexibility (Camenzind et al., 2021).

Additionally, we explored the consequences of C overflow as DOC as opposed to CO_2 by redirecting this flux to a pool of monomers containing only C. We chose the pool of hemicellulose monomers for this purpose. Finally, as microbial population dynamics can also play a role in solving elemental imbalance, we manipulated the microbial community by establishing two community contexts. In the first, meant to represent high functional redundancy, the community was represented by a single taxon possessing all 12 enzymes. The second community context was composed of 100 taxa, each possessing s 0 to 12 different enzymes. To ensure a fair representation of the range of degrading capabilities, we first calculated all possible enzyme combinations for each category (Table 3). Combinations with 0, 1, 11, and 12 enzymes were fully represented due to the low number of possible combinations. For the other categories, we randomly selected some of the combinations.

With the manipulation of community context, overflow nature, biomass stoichiometry, and nutrient allocation, our control scenario corresponds to a 1 taxon community with overflow as CO_2, fixed stoichiometry and no nutrient allocation. This scenario depicts the expected outcome of overflow respiration alone. We performed a total of 1,944 simulations (81 different

https://doi.org/10.5194/egusphere-2026-3590
Preprint. Discussion started: 30 June 2026

initial litter C:N, 2 community contexts, 2 overflow types, 2 biomass stoichiometry scenarios, and 3 nutrient allocation scenarios).

Table 2. Simulation setup

Initial litter C:N	Community context	Overflow	Stoichiometry	Nutrient allocation
10–90	High redundancy (1 taxon)	CO_2	Fixed	None
				Enzyme
				Enzyme + Uptake
			Flexible	None
				Enzyme
				Enzyme + Uptake
		DOC	Fixed	None
				Enzyme
				Enzyme + Uptake
			Flexible	None
				Enzyme
				Enzyme + Uptake
	Low redundancy (100 taxa)	CO_2	Fixed	None
				Enzyme
				Enzyme + Uptake
			Flexible	None
				Enzyme
				Enzyme + Uptake
		DOC	Fixed	None
				Enzyme
				Enzyme + Uptake
			Flexible	None
				Enzyme
				Enzyme + Uptake

https://doi.org/10.5194/egusphere-2026-3590
Preprint. Discussion started: 30 June 2026

Table 3. Determination of microbial degrading capabilities for the low redundancy community context (100 taxa)

Nº Enzymes	Nº Combinations	Nº Taxa
0	1	1
1	12	12
2	66	8
3	220	8
4	495	8
5	792	9
6	924	9
7	792	8
8	495	8
9	220	8
10	66	8
11	12	12
12	1	1

2.5 Analysis of model output

To test the consequences of our mechanisms, we computed aggregated metrics of key variables across the range of litter C:N manipulations. By aggregated metric, we mean a single computed value that represents the entire decomposition process of a specific litter cohort. To ensure consistency, we standardize all our simulations, considering decomposition up to 50% C mass loss. The carbon-use efficiency of a single simulation was computed as:

$$CUE = \frac{\sum_1^{999} U_C - R}{\sum_1^{999} U_C} \quad (5)$$

where R corresponds to the total microbial respiration (mg CO_2 cm^{-2} day^{-1}), and U_C is the total C uptake (mg C cm^{-2} day^{-1}) at that time-step. This definition considers only CO_2 as C loss. Although enzymes are secreted to the environment, they constitute a C pool that is still part of the soil system and can be used again by microbes as a C source. By plotting carbon-use efficiency as a function of initial litter C:N we assess the control of litter stoichiometry on soil C losses.

https://doi.org/10.5194/egusphere-2026-3590
Preprint. Discussion started: 30 June 2026

3. Results

Imposing overflow respiration results in a very specific response of carbon-use efficiency to elemental imbalance (i.e., initial litter C:N). This relationship is usually characterized by constant, high carbon-use efficiency values for low C:N litter until reaching N limitation, beyond which point carbon-use efficiency starts to decline (blue solid line in Fig. 4a). We found that this pattern was considerably affected by 1) the nature of overflow (i.e., CO_2 vs DOC), 2) the physiological mechanisms involved in elemental imbalance acclimation, and 3) the functional diversity of the community.

3.1 Flexible stoichiometry avoids overflow, unlike nutrient allocation

As alternatives to overflow, we introduced other physiological mechanisms that contribute to reducing elemental imbalance, including flexible stoichiometry and nutrient allocation (enzyme and/or uptake allocation). For scenarios with flexible biomass stoichiometry we did not observe any decrease in carbon-use efficiency with higher litter C:N (Fig. 4a). We can also attribute this result to a lack of overflow respiration (Fig. S1). Nevertheless, the introduction of nutrient allocation strategies did not prevent overflow (Fig. 4a). Although our introduced mechanism of enzyme and uptake allocation does modulate enzyme and uptake dynamics (Fig. S2), it is not sufficient to avoid overflow respiration. However, nutrient allocation in the form of both enzyme and uptake allocation caused higher values of carbon-use efficiency for litter C:N < 50. This increase was particularly evident when biomass stoichiometry was fixed (solid black line in Fig. 4a). Elevated carbon-use efficiency was caused by lower total respiration values (Fig. 5a), which in turn were caused by lower maintenance respiration (Fig. S3a).

3.2 The nature of C overflow matters for C losses

When we redirected C-overflow from CO_2 to DOC, carbon-use efficiency increased upon reaching N limitation (Fig. 4b). This pattern was observed only in the scenarios with observed overflow (i.e., when C was the element in excess). Since overflow respiration did not happen when biomass stoichiometry was allowed to fluctuate, these simulations showed little variation in carbon-use efficiency with DOC overflow, following the same dynamics as with CO_2 overflow. The increase in carbon-use efficiency due to DOC overflow seemed to be proportional to the amount of overflow, as inferred from the quasi-symmetry with the simulations with CO_2 overflow. Although this increase might appear intuitive due to all the C that was redirected from CO_2, DOC overflow caused a reduction in total respiration of 3 to 9% (Fig. 5a), which is insufficient to explain the increase in carbon-use efficiency (Eq. (5)). Rather, the increase was mainly due to higher uptake (Fig. S4a) of the extra DOC from overflow itself (C recycling). Even though DOC overflow prevents excess C from being lost as CO_2, the reduction in total respiration is less than the reduction in CO_2 overflow. The reason is that higher C uptake translates into higher growth respiration (Eq. (A10), left panels of Fig. 6), counteracting the reduction in overflow respiration.

https://doi.org/10.5194/egusphere-2026-3590
Preprint. Discussion started: 30 June 2026

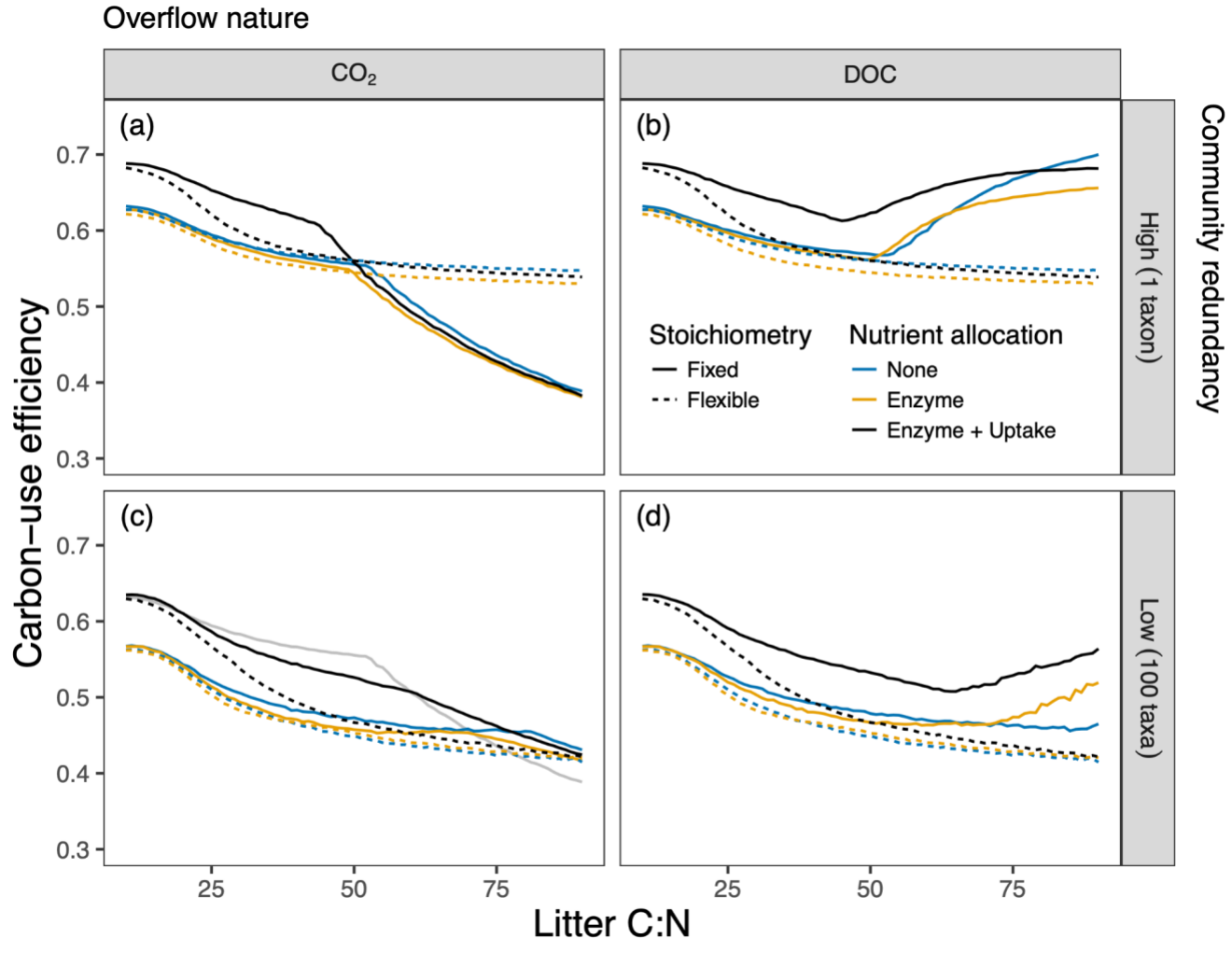

Figure 4. Carbon-use efficiency in response to initial litter C:N. Vertical panels separate simulations by CO_2 or DOC overflow. Horizontal panels distinguish high (1 taxon) and low (100 taxa) redundancy community contexts. Colors represent scenarios of nutrient allocation. Line dash indicates biomass stoichiometry flexibility. The "overflow only" simulation in (a) (solid blue line) is reprinted in (c) as a solid gray line for comparison.

Similarly to simulations with CO_2 overflow, allowing for enzyme and uptake allocation when stoichiometry is fixed caused high carbon-use efficiency values (Fig. 4b). This time though, the effect remained at high litter C:N since there was no reduction in carbon-use efficiency due to overflow respiration. Additionally, any form of nutrient allocation (i.e., enzyme or enzyme plus uptake allocation) caused an increase in maintenance respiration at litter C:N > 50 (Fig. 6c, e) driven by higher enzyme production (Fig. S5b).

https://doi.org/10.5194/egusphere-2026-3590
Preprint. Discussion started: 30 June 2026

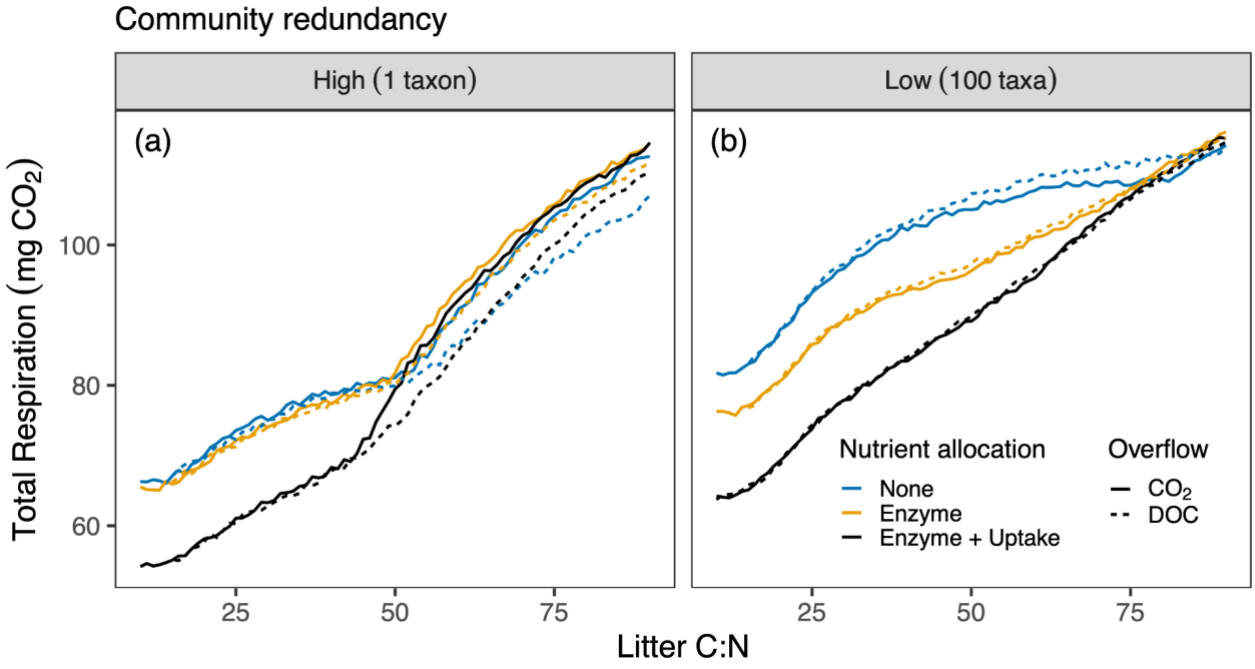

Figure 5. Total respiration (mg CO_2 cm-2) after 50% of C mass loss as a function of initial litter C:N. Colors represent scenarios of nutrient allocation. Solid lines indicate overflow as CO_2, dashed lines indicate overflow as DOC. Simulations with flexible biomass stoichiometry were not included due to the lack of observed C overflow.

3.3 A diverse community reduces C overflow but increases maintenance

In the low redundancy community (100 taxa) there was no evidence of reduced carbon-use efficiency due to overflow (Fig. 4c). Figure S1c also confirms that overflow was lower than for the high redundancy community and occurred only at litter C:N > 50, indicating that most of these simulations were C-limited. Indeed, the diverse community exhibited higher levels of nitrogen uptake, particularly from necromass (Fig. S6c-d). Greater necromass nutrient recycling is evident in this community due in part to higher necromass production (Fig. S7c-d).

Despite the reduction in overflow respiration, carbon-use efficiency remained at lower values than for the high redundancy community throughout most of the litter C:N range. These lower values were not explained by lower C uptake (Fig. S4b) but rather higher total respiration (Fig. 5b) largely driven by higher maintenance respiration (Fig. S3b). Maintenance respiration depends on enzyme and transporter production (Eq. (A11)). Total enzyme production was lower than for the high redundancy community (Fig. S5c-d). Therefore, we attribute higher maintenance to higher transporter biomass. While we cannot retrieve this quantity directly, total microbial biomass was higher for the low redundancy community (Fig. S8).

https://doi.org/10.5194/egusphere-2026-3590
Preprint. Discussion started: 30 June 2026

Having a diverse community also changes the effect of DOC overflow. In our 100-taxa community, redirecting C overflow from CO_2 to DOC resulted in a subtle increase in total respiration (Fig. 5b). This small increase can be explained by a lower amount of C overflow, which means less C being recycled as DOC. This low C recycling is in turn insufficient to counteract the increases in growth and maintenance respiration (right panels of Fig. 6).

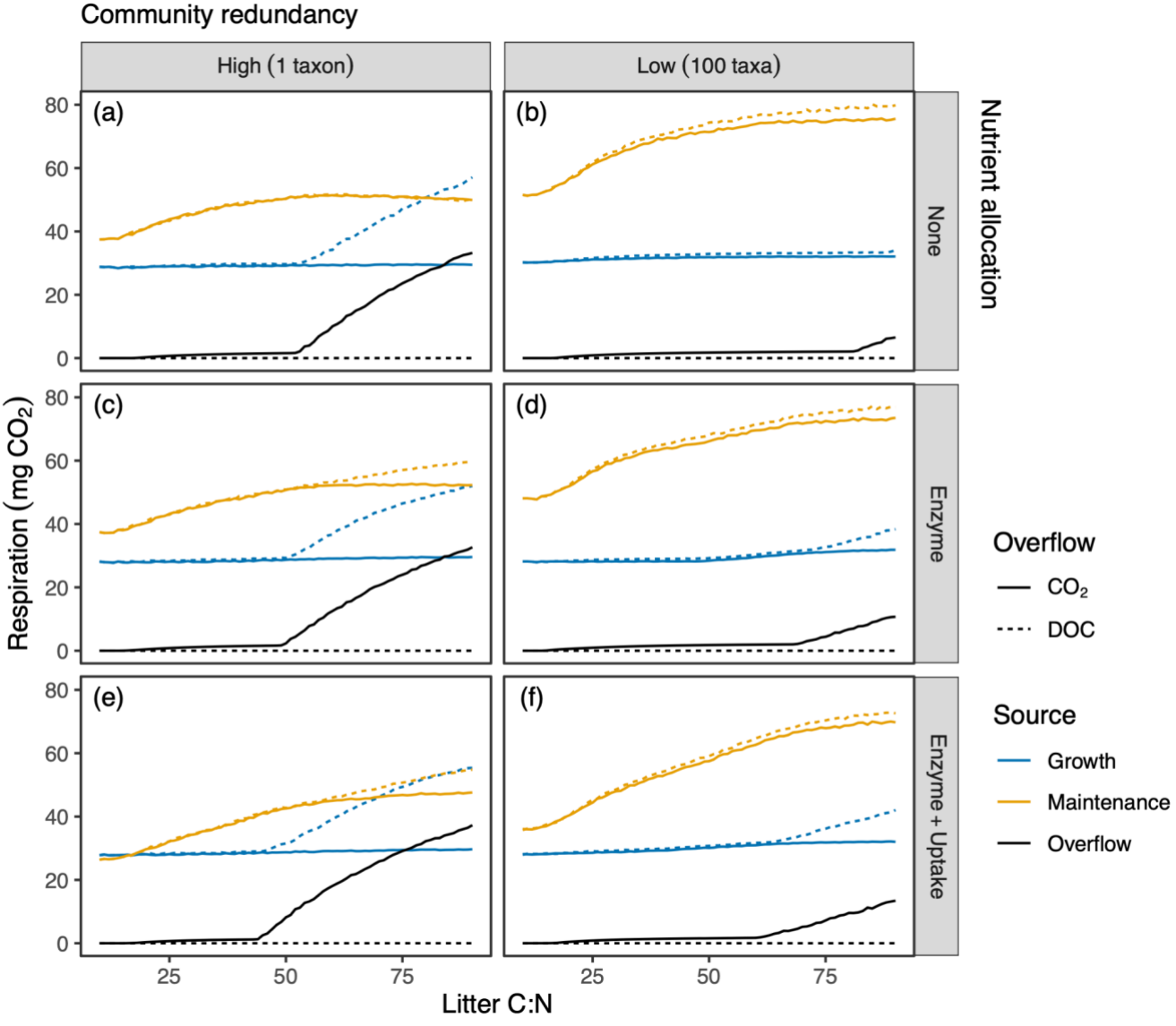

Figure 6. Respiration components (mg CO_2 cm-2) after 50% of C mass loss as a function of initial litter C:N. Total respiration is decomposed into its sources represented by different colors. Vertical panels separate simulations by community context. Horizontal panels distinguish between scenarios of nutrient allocation. Solid lines indicate overflow as CO_2, dashed lines indicate overflow as DOC. Simulations with flexible biomass stoichiometry were excluded from this figure due to their lack of (realized) C overflow.

https://doi.org/10.5194/egusphere-2026-3590
Preprint. Discussion started: 30 June 2026

4. Discussion

Overflow respiration in soil C models may force a decrease in microbial carbon-use efficiency when decomposers feed on high C:N plant litter. We propose that such declines in carbon-use efficiency may be mitigated by three non-mutually exclusive mechanisms: 1) physiological acclimation to elemental imbalances that avoid C overflow, 2) overflow as DOC instead of CO_2, and 3) functional diversity in microbial communities that improves nutrient recycling. We tested the consequences of these mechanisms on emergent carbon-use efficiency using a complex microbial-based model. We found that all three mechanisms have an impact on carbon-use efficiency, although the direction and magnitude depend on the mechanism. Overall, we found that flexible biomass stoichiometry avoided overflow, while nutrient allocation did not. DOC overflow increased carbon-use efficiency instead of decreasing it like CO_2 overflow. Finally, a functionally diverse community can avoid overflow, but yields lower carbon-use efficiency due to high maintenance.

4.1 Physiological acclimation to elemental imbalance

We observed that flexible biomass stoichiometry avoided C overflow, but nutrient allocation strategies did not. DEMENT assumes that microbes maintain stoichiometric homeostasis by excreting excess elements (Eq. (A5) to Eq. (A8)). By introducing flexible biomass stoichiometry, the elemental quotas of the biomass are allowed to fluctuate within a tolerance range. Provided that these quotas stay within that range, there will be no excess and therefore, no overflow. In other words, flexible biomass stoichiometry in DEMENT completely solves elemental imbalance. This is of course dependent on the tolerance range. We informed our tolerance range by data from fungal isolates with high biomass stoichiometry flexibility (Camenzind et al., 2021). The narrower the flexibility, the higher the chance of C excess, and therefore, overflow. Biomass flexibility could potentially become a trait to be parametrized.

On the other hand, our newly introduced mechanism for enzyme and uptake allocation, although regulated by nutrient availability, does not fully mitigate elemental imbalance. This result contrasts with previous model formulations based on optimal enzyme allocation (Averill, 2014; Moorhead et al., 2012; Wutzler et al., 2017). Our approach is based on mechanistic understanding of gene regulation and is computationally less expensive than previous approaches. Furthermore, those other studies assumed a much simpler 2-polymer system. The 12 polymers in DEMENT and their diverse elemental composition create further constraints on an optimal solution of elemental imbalance. Data from fungal isolates grown in minimal media also support regulation of enzyme production, but this regulation does not completely solve elemental imbalance (manuscript under review). Although nutrient allocation is likely a universal mechanism to decrease elemental imbalance (Leigh & Dodsworth, 2007; Magasanik & Kaiser, 2002; Thomas & O'Shea, 2005; Wanner, 1993), it may be insufficient to prevent overflow fluxes. Unlike biomass stoichiometry, the "level" of nutrient allocation could be more challenging to parametrize.

https://doi.org/10.5194/egusphere-2026-3590
Preprint. Discussion started: 30 June 2026

4.2 DOC overflow and the representation of respiratory processes in soil C models

Our simulations with DOC overflow increased carbon-use efficiency under nitrogen-limited conditions, mainly due to higher C uptake of additional DOC. This additional uptake, however, also increased growth respiration. The net effect on total respiration is mainly dependent on the assimilation efficiency (e in Eq. (A10)). The assimilation efficiency controls how much CO_2 is produced from C uptake. The higher the assimilation efficiency, the lower the growth respiration and the higher the reduction in total respiration from DOC relative to CO_2 overflow.

This finding highlights the importance of revisiting the way we represent respiration processes in models. One of the advantages of DEMENT is its representation of CO_2 production by different cellular processes (growth, enzyme production, overflow, etc.). Previous studies have argued against representing carbon-use efficiency as a single parameter (Hagerty et al., 2018). Although the mechanistic architecture of DEMENT enables us to explore the causes of carbon-use efficiency changes, features like a fixed assimilation efficiency are still unrealistic (Gommers et al., 1988) and may introduce biases.

Additionally, our implementation of DOC overflow involves a pre-existing C monomer (monomer of hemicellulose) for convenience. The exact monomer selected for this purpose did not matter as long as it contained only C. Empirical studies have characterized overflow metabolism mostly as the excretion of organic acids (Chowdhury et al., 2025; Neijssel & Tempest, 1975). These compounds have a lower energetic content than other C sources like the sugars that comprise hemicellulose (LaRowe & Van Cappellen, 2011). DEMENT does not represent energy fluxes, and an energy-explicit model would enable a more accurate representation of respiratory processes and acknowledging the vast chemo-diversity of soils (Ding et al., 2020; Roth et al., 2019). A more rigorous assessment of DOC overflow would require both mass and energy constraints in carbon-use efficiency.

4.3 The impact of microbial functional diversity

Simulations with functionally diverse communities (i.e., varying polymer-degrading capabilities among taxa) exhibited a reduction in overflow respiration. Nevertheless, carbon-use efficiency remained low due to higher transporter production respiration. Microbial interactions across functionally distinct taxa are usually neglected in most soil C models. However, these higher-level mechanisms can exert a strong control on ecosystem functions (Bertolet et al., 2024). From previous *in silico* experiments we know that population dynamics of plant and necromass decomposer specialists lead to a higher nutrient recycling rate (Kaiser et al., 2014). Although we did not observe the succession dynamics reported in that study, we did observe higher nutrient recycling from necromass, which can help explain decreased overflow respiration in this community.

https://doi.org/10.5194/egusphere-2026-3590
Preprint. Discussion started: 30 June 2026

Varying microbial degrading capabilities of taxa implies reducing maintenance costs. Since the average number of enzymes possessed by a taxon is lower in our 100 taxa community, maintenance costs associated with enzyme production are also lower. Nevertheless, all taxa possessed all transporter types. Since total biomass was higher in this community than in the 1 taxon community, total transporter biomass was higher. This higher transporter biomass yielded higher maintenance respiration in spite of the reduction in enzyme costs.

Additionally, representing a diverse community is relevant for assessing the full impact of mechanisms that reduce nutrient imbalance. In nature, DOC overflow can have an impact in cross-feeding interactions, especially considering the tradeoff between sugar and organic acid preferences as C source (Gralka et al., 2023). Moreover, physiological mechanisms like flexible biomass stoichiometry might be highly variable across taxa (Camenzind et al., 2021; Mouginot et al., 2014). This variability could have consequences for performance when microbes interact in a diverse community. One of the limitations of our simulations is that we did not implement our mechanisms in specific taxa. Such an approach would be needed to test competitive advantages of specific mechanisms.

4.4 Implications for modeling

Previous studies demonstrate how different mechanisms to solve elemental imbalance lead to differences in C and N mineralization (Fujita et al., 2014; Manzoni et al., 2021; Manzoni & Porporato, 2009; Wutzler et al., 2017). Fujita et al. (2014) validated different soil organic matter decomposition models using C and N mineralization data from laboratory incubation experiments. They found that overflow respiration outperformed N inhibition of decomposition, the latter leading to underestimation of C and N mineralization. Nevertheless, validation approaches can still lead to equifinality (i.e., observations could be explained by more than one mechanism) as noted by Manzoni et al. (2021). Although formal validation is still needed, we advocate starting from well characterized physiological mechanisms, since overflow respiration largely lacks empirical support (but see Spohn, 2015). To our knowledge, we are the first study to test the effects of dissolved organic C overflow and to assess different mechanisms of coping with elemental imbalance co-occurring in the same simulation. However, for bigger scales, some of the complexity introduced in our simulations must be ignored to reduce computational effort.

Implementing some of the mechanisms we tested in an earth-system model would be impractical. In particular, analytical solutions of nutrient allocation require significant computational effort compared to the simple overflow respiration mechanism (Moorhead et al., 2012; Wutzler et al., 2017). However, our heuristic sigmoid curve could be a “cheaper” option. Flexible biomass stoichiometry seems to be species-dependent (Camenzind et al., 2021) and would require more data to correctly parametrize this mechanism. Moreover, its implementation may not improve predictions (Fujita et al., 2014). The

https://doi.org/10.5194/egusphere-2026-3590
Preprint. Discussion started: 30 June 2026

easiest implementation would be to redirect C overflow from CO_2 to dissolved organic C. These are pools already present in a soil organic matter decay model, consequently, no extra computational power is needed. Yet, as we note from our results, this flux redirection could lead to major differences in C mineralization.

4.5 Conclusions

Despite the ubiquity of overflow respiration in soil C models, we demonstrate that it may have unrealistic consequences. The associated reduction in carbon-use efficiency due to CO_2 overflow is unrealistic because overflow might commonly occur as DOC, which increases carbon-use efficiency instead of decreasing it. Moreover, physiological acclimation to elemental imbalances via nutrient allocation or flexible biomass stoichiometry has the potential to avoid overflow by solving the imbalance before C excretion happens. In addition, functional diversity in microbial communities can improve nutrient recycling and reduce C overflow, although with potential unexpected effects on carbon-use efficiency. For future model improvements of models with overflow respiration, the easiest solution would be to redirect C overflow into DOC. Physiological acclimation and functional diversity are computationally expensive to implement, especially in higher-scale models (e.g., soil compartment in an earth-system model). We also expect to see future tests of these mechanisms considering energetic and chemo-diversity aspects. The findings of this study could potentially improve the predictive power of soil biogeochemical models.

Appendix A

Here we include definitions of some of the major processes in DEMENT:

Decomposition

The decay of a given polymer into its constituent monomers is mediated by one enzyme (in our case) through forward Michaelis-Menten kinetics

$$Decay = (E \times V_{max}) \times \frac{S_P}{K_m + S_P} \quad \text{(A1)}$$

Where E is the enzyme concentration, V_{max} is the maximum velocity of the reaction, K_m is the half saturation constant of the reaction, and S_P is the polymer concentration. The sum of the decay of all polymers yields the litter decomposition rate.

https://doi.org/10.5194/egusphere-2026-3590
Preprint. Discussion started: 30 June 2026

Uptake

The uptake of monomers produced by extracellular enzyme activity is mediated by transmembrane transporters following forward Michaelis-Menten kinetics. Uptake for a given monomer is calculated as:

$$Uptake = (U_A \times B) \times (V_{max} \times \frac{S_M}{K_m + S_M}) \quad \text{(A2)}$$

Where U_A is the uptake allocation, the proportion of biomass allocated to the transporters; B is the microbial biomass of a given taxon; and S_M is the monomer concentration. Each monomer has a defined C:N:P stoichiometry (Table 1).

Growth

The amount of C available to build new biomass is determined by:

$$C_G = (C_U \times e) - C_E - R_M \quad \text{(A3)}$$

Where C_U is the total C uptake, e is the assimilation efficiency, C_E is the C secreted as extracellular enzymes, and R_M is the amount of respiration (CO_2) attributed to maintenance (see below).

Enzyme production

Extracellular enzyme production is given by:

$$E_{prod} = C_U \times E_{ind} + B \times E_{const} \quad \text{(A4)}$$

Where E_{ind} is the proportion of C uptake used in enzyme production which we call "induced" production, and E_{const} is a proportion of biomass (B) allocated to enzyme production (independent of C uptake) that we refer to as "constitutive" production. E_{prod} is constrained by the available N in the biomass.

Biomass stoichiometry homeostasis and excretion

Microbes have a minimum quota (Q_{min}) of C, N, and P (expressed as a fraction of total biomass). In each timestep, microbes that have quotas below the minimum value are identified. The magnitude of the deficit is calculated for each element for each microbe.

$$Deficit = (Q_{min} - Q) > 0 \quad \text{(A5)}$$

https://doi.org/10.5194/egusphere-2026-3590
Preprint. Discussion started: 30 June 2026

$$Excess = (Q_{min} - Q) < 0 \quad \text{(A6)}$$

The element with the highest deficit is selected as the "limiting" element, which will be conserved (following Liebig's law)

$$Limiting = max[\frac{Q_{min} - Q}{Q_{min}}] \quad \text{(A7)}$$

Where Q is the current quota. The quotas of deficient elements are set to their minima. Quotas of non-deficient (excess) elements are reduced in proportion to their distance to the minimum quota

$$\dot{Q_E} = Q_E - \frac{(\sum Deficit) \times Excess}{\sum Excess} \quad \text{(A8)}$$

Where Q_E is the quota of the element in excess. Hypothetical quotas of each element are calculated for each possible limiting element. The absolute amounts of microbial C, N, and P are recalculated based on the newly calculated quotas. The amount of the limiting element is conserved as it is. The amount of a non-limiting element is calculated with the amount of the limiting element times the ratio between the quota of the element in question over the quota of the limiting element.

Respiration

Total respiration (R) is partitioned into growth (R_G), maintenance (R_M), and overflow (R_G):

$$R = R_G + R_M + R_O \quad \text{(A9)}$$

Growth respiration is given by:

$$R_G = C_U \times (1 - e) \quad \text{(A10)}$$

Maintenance respiration is given by:

$$R_M = R_E + R_U \quad \text{(A11)}$$

Where R_E is the respiration produced in enzyme production, and R_U is the respiration produced in transporter production:

https://doi.org/10.5194/egusphere-2026-3590
Preprint. Discussion started: 30 June 2026

$$R_E = E_{prod} \times M_E \quad \text{(A12)}$$

$$R_U = (U_A \times B) \times M_U \quad \text{(A13)}$$

Where M_E and M_U are the maintenance costs associated with producing enzymes and transporters respectively.

Microbial death

Death is driven by two processes, a deterministic one, which is starvation, and a stochastic one. Stochastic death is determined by a death rate parameter (% per time step). Starvation is defined in minimum biomass requirements for each element (C_{min} , N_{min} , P_{min}). Unlike the minimum quotas, these quantities are defined in absolute mass. If the elemental content of biomass decreases below any of these thresholds, the microbe dies of starvation.

Enzyme inactivation

Enzymes have a turnover rate defined by the enzyme loss rate (ϵ). Enzyme inactivation is given by:

$$E_{loss} = E \times \epsilon \quad \text{(A14)}$$

ϵ determines the proportion of enzymes that are inactivated per time step. The enzyme loss rate is multiplied by the total pool of enzymes (E) to determine the amount of enzymes that are added to the "inactive enzyme" pool each time step (E_{loss}).

Code and data availability

Data and code to reproduce the figures can be found at the Dryad repository: http://datadryad.org/share/LINK_NOT_FOR_PUBLICATION/rwVHybNZ2Q6QwtXEG9L78vgKl4xQi3mAay5Hh9sRZZc

Code and instructions to reproduce the simulations from scratch can be found in GitHub, with the following Zenodo DOI: 10.5281/zenodo.20752610

https://doi.org/10.5194/egusphere-2026-3590
Preprint. Discussion started: 30 June 2026

Author contributions

The study was conceptualized by JM and SA. All co-authors discussed simulation layout and specifications. JM modified the model with critical inputs from all co-authors. JM ran all simulations, processed the outputs, and generated the figures. JM prepared the manuscript with review and edits from all co-authors. All co-authors contributed to the discussion and interpretation of results. SA was involved in funding acquisition.

Competing interests

The authors declare no conflict of interest.

Acknowledgements

We would like to thank Elsa Abs, Stefano Manzoni, María Rebolleda-Gomez, Jonathan Donhauser, Amilcare Porporato, and Albert Brangarí for fruitful discussions about modelling microbial physiology and organic matter decomposition. We also extend our gratitude to the members of work-package-2 from the CALIPSO project for their useful comments in earlier stages of the study. We are grateful to UC Irvine's High Performance Computing Cluster and associated staff for making our simulations possible.

Financial support

This study was funded by Schmidt Sciences through the CALIPSO project

References

Abramoff, R. Z., Davidson, E. A., and Finzi, A. C.: A parsimonious modular approach to building a mechanistic belowground carbon and nitrogen model, J. Geophys. Res. Biogeosci., https://doi.org/10.1002/2017JG003796, 2017.

Allison, S. D.: A trait-based approach for modelling microbial litter decomposition, Ecol. Lett., 15, 1058–1070, https://doi.org/10.1111/j.1461-0248.2012.01807.x, 2012.

https://doi.org/10.5194/egusphere-2026-3590
Preprint. Discussion started: 30 June 2026

Allison, S. D.: Modeling adaptation of carbon use efficiency in microbial communities, Front. Microbiol., 5, 571, https://doi.org/10.3389/fmicb.2014.00571, 2014.

Allison, S. D. and Goulden, M. L.: Consequences of drought tolerance traits for microbial decomposition in the DEMENT model, Soil Biol. Biochem., 107, 104–113, https://doi.org/10.1016/j.soilbio.2017.01.001, 2017.

Allison, S. D., Wallenstein, M. D., and Bradford, M. A.: Soil-carbon response to warming dependent on microbial physiology, Nat. Geosci., 3, 336–340, https://doi.org/10.1038/ngeo846, 2010.

Averill, C.: Divergence in plant and microbial allocation strategies explains continental patterns in microbial allocation and biogeochemical fluxes, Ecol. Lett., 17, 1202–1210, https://doi.org/10.1111/ele.12324, 2014.

Bertolet, B. L., Rodriguez, L. C., Murúa, J. M., Favela, A., and Allison, S. D.: The impact of microbial interactions on ecosystem function intensifies under stress, Ecol. Lett., 27, e14528, https://doi.org/10.1111/ele.14528, 2024.

Boberg, J., Finlay, R., Stenlid, J., Nasholm, T., and Lindahl, B.: Glucose and ammonium additions affect needle decomposition and carbon allocation by the litter degrading fungus Mycena epipterygia, Soil Biol. Biochem., 40, 995–999, https://doi.org/10.1016/j.soilbio.2007.11.005, 2008.

Bonachela, J. A., Allison, S. D., Martiny, A. C., and Levin, S. A.: A model for variable phytoplankton stoichiometry based on cell protein regulation, Biogeosciences, 10, 4341–4356, https://doi.org/10.5194/bg-10-4341-2013, 2013.

Bosatta, E. and Berendse, F.: Energy or nutrient regulation of decomposition: Implications for the mineralization-immobilization response to perturbations, Soil Biol. Biochem., 16, 63–67, https://doi.org/10.1016/0038-0717(84)90127-5, 1984.

Camenzind, T., Philipp Grenz, K., Lehmann, J., and Rillig, M. C.: Soil fungal mycelia have unexpectedly flexible stoichiometric C:N and C:P ratios, Ecol. Lett., 24, 208–218, https://doi.org/10.1111/ele.13632, 2021.

Chowdhury, N. B., Schroeder, W. L., Monteiro, L., and Burnum-Johnson, K. E.: mGem: Revisiting bacterial overflow metabolism, MBio, 16, e0119325, https://doi.org/10.1128/mbio.01193-25, 2025.

Ding, Y., Shi, Z., Ye, Q., Liang, Y., Liu, M., Dang, Z., Wang, Y., and Liu, C.: Chemodiversity of soil dissolved organic matter, Environ. Sci. Technol., 54, 6174–6184, https://doi.org/10.1021/acs.est.0c01136, 2020.

Folse, H. J., 3rd and Allison, S. D.: Cooperation, competition, and coalitions in enzyme-producing microbes: social evolution and nutrient depolymerization rates, Front. Microbiol., 3, 338, https://doi.org/10.3389/fmicb.2012.00338, 2012.

Fontaine, S. and Barot, S.: Size and functional diversity of microbe populations control plant persistence and long-term soil carbon accumulation, Ecol. Lett., 8, 1075–1087, https://doi.org/10.1111/j.1461-0248.2005.00813.x, 2005.

Fujita, Y., Witte, J.-P. M., and van Bodegom, P. M.: Incorporating microbial ecology concepts into global soil mineralization models to improve predictions of carbon and nitrogen fluxes, Global Biogeochem. Cycles, 28, 223–238, https://doi.org/10.1002/2013gb004595, 2014.

Gommers, P. J., van Schie, B. J., van Dijken, J. P., and Kuenen, J. G.: Biochemical limits to microbial growth yields: An analysis of mixed substrate utilization, Biotechnol. Bioeng., 32, 86–94, https://doi.org/10.1002/bit.260320112, 1988.

https://doi.org/10.5194/egusphere-2026-3590
Preprint. Discussion started: 30 June 2026

Gralka, M., Pollak, S., and Cordero, O. X.: Genome content predicts the carbon catabolic preferences of heterotrophic bacteria, Nat. Microbiol., 8, 1799–1808, https://doi.org/10.1038/s41564-023-01458-z, 2023.

Hadas, A., Parkin, T. B., and Stahl, P. D.: Reduced CO 2 release from decomposing wheat straw under N-limiting conditions: simulation of carbon turnover, Eur. J. Soil Sci., 49, 487–494, https://doi.org/10.1046/j.1365-2389.1998.4930487.x, 1998.

Hagerty, S. B., Allison, S. D., and Schimel, J. P.: Evaluating soil microbial carbon use efficiency explicitly as a function of cellular processes: implications for measurements and models, Biogeochemistry, 140, 269–283, https://doi.org/10.1007/s10533-018-0489-z, 2018.

Huang, Y., Guenet, B., Ciais, P., Janssens, I. A., Soong, J. L., Wang, Y., Goll, D., Blagodatskaya, E., and Huang, Y.: ORCHIMIC (v1.0), a microbe-mediated model for soil organic matter decomposition, Geosci. Model Dev., 11, 2111–2138, https://doi.org/10.5194/gmd-11-2111-2018, 2018.

Kaiser, C., Franklin, O., Dieckmann, U., and Richter, A.: Microbial community dynamics alleviate stoichiometric constraints during litter decay, Ecol. Lett., 17, 680–690, https://doi.org/10.1111/ele.12269, 2014.

Kersebaum, K. C. and Richter, O.: A model approach to simulate C and N transformations through microbial biomass, Eur. J. Agron., 3, 355–360, https://doi.org/10.1016/s1161-0301(14)80166-4, 1994.

Kyker-Snowman, E., Wieder, W. R., Frey, S. D., and Grandy, A. S.: Stoichiometrically coupled carbon and nitrogen cycling in the MIcrobial-MIneral Carbon Stabilization model version 1.0 (MIMICS-CN v1.0), Geosci. Model Dev., 13, 4413–4434, https://doi.org/10.5194/gmd-13-4413-2020, 2020.

LaRowe, D. E. and Van Cappellen, P.: Degradation of natural organic matter: A thermodynamic analysis, Geochim. Cosmochim. Acta, 75, 2030–2042, https://doi.org/10.1016/j.gca.2011.01.020, 2011.

Leigh, J. A. and Dodsworth, J. A.: Nitrogen regulation in bacteria and archaea, Annu. Rev. Microbiol., 61, 349–377, https://doi.org/10.1146/annurev.micro.61.080706.093409, 2007.

Li, J., Wang, G., Allison, S. D., Mayes, M. A., and Luo, Y.: Soil carbon sensitivity to temperature and carbon use efficiency compared across microbial-ecosystem models of varying complexity, Biogeochemistry, 119, 67–84, https://doi.org/10.1007/s10533-013-9948-8, 2014.

Logan, J. D., Joern, A., and Wolesensky, W.: Control of CNP homeostasis in herbivore consumers through differential assimilation, Bull. Math. Biol., 66, 707–725, https://doi.org/10.1016/j.bulm.2003.10.008, 2004.

Magasanik, B. and Kaiser, C. A.: Nitrogen regulation in Saccharomyces cerevisiae, Gene, 290, 1–18, https://doi.org/10.1016/s0378-1119(02)00558-9, 2002.

Manzoni, S. and Porporato, A.: Soil carbon and nitrogen mineralization: Theory and models across scales, Soil Biol. Biochem., 41, 1355–1379, https://doi.org/10.1016/j.soilbio.2009.02.031, 2009.

Manzoni, S., Taylor, P., Richter, A., Porporato, A., and Ågren, G. I.: Environmental and stoichiometric controls on microbial carbon-use efficiency in soils, New Phytol., 196, 79–91, https://doi.org/10.1111/j.1469-8137.2012.04225.x, 2012.

https://doi.org/10.5194/egusphere-2026-3590
Preprint. Discussion started: 30 June 2026

Manzoni, S., Chakrawal, A., Spohn, M., and Lindahl, B. D.: Modeling microbial adaptations to nutrient limitation during litter decomposition, Front. For. Glob. Chang., 4, https://doi.org/10.3389/ffgc.2021.686945, 2021.

Moorhead, D. L., Lashermes, G., and Sinsabaugh, R. L.: A theoretical model of C- and N-acquiring exoenzyme activities, which balances microbial demands during decomposition, Soil Biol. Biochem., 53, 133–141, https://doi.org/10.1016/j.soilbio.2012.05.011, 2012.

Mouginot, C., Kawamura, R., Matulich, K. L., Berlemont, R., Allison, S. D., Amend, A. S., and Martiny, A. C.: Elemental stoichiometry of Fungi and Bacteria strains from grassland leaf litter, Soil Biol. Biochem., 76, 278–285, https://doi.org/10.1016/j.soilbio.2014.05.011, 2014.

Neijssel, O. M. and Tempest, D. W.: The regulation of carbohydrate metabolism in Klebsiella aerogenes NCTC 418 organisms, growing in chemostat culture, Arch. Microbiol., 106, 251–258, https://doi.org/10.1007/bf00446531, 1975.

Raynaud, X., Lata, J.-C., and Leadley, P. W.: Soil microbial loop and nutrient uptake by plants: a test using a coupled C:N model of plant–microbial interactions, Plant Soil, 287, 95–116, https://doi.org/10.1007/s11104-006-9003-9, 2006.

Roth, V.-N., Lange, M., Simon, C., Hertkorn, N., Bucher, S., Goodall, T., Griffiths, R. I., Mellado-Vázquez, P. G., Mommer, L., Oram, N. J., Weigelt, A., Dittmar, T., and Gleixner, G.: Persistence of dissolved organic matter explained by molecular changes during its passage through soil, Nat. Geosci., 12, 755–761, https://doi.org/10.1038/s41561-019-0417-4, 2019.

Schimel, J. and Weintraub, M. N.: The implications of exoenzyme activity on microbial carbon and nitrogen limitation in soil: a theoretical model, Soil Biol. Biochem., 35, 549–563, https://doi.org/10.1016/s0038-0717(03)00015-4, 2003.

Shaffer, M. J., Halvorson, A. D., and Pierce, F. J.: Nitrate leaching and economic analysis package (NLEAP): Model description and application, in: Managing Nitrogen for Groundwater Quality and Farm Profitability, Soil Science Society of America, Madison, WI, USA, 285–322, https://doi.org/10.2136/1991.managingnitrogen.c13, 2015.

Sistla, S. A., Rastetter, E. B., and Schimel, J. P.: Responses of a tundra system to warming using SCAMPS: a stoichiometrically coupled, acclimating microbe–plant–soil model, Ecol. Monogr., 84, 151–170, https://doi.org/10.1890/12-2119.1, 2014.

Spohn, M.: Microbial respiration per unit microbial biomass depends on litter layer carbon-to-nitrogen ratio, Biogeosciences, 12, 817–823, https://doi.org/10.5194/bg-12-817-2015, 2015.

Tao, F., Huang, Y., Hungate, B. A., Manzoni, S., Frey, S. D., Schmidt, M. W. I., Reichstein, M., Carvalhais, N., Ciais, P., Jiang, L., Lehmann, J., Wang, Y.-P., Houlton, B. Z., Ahrens, B., Mishra, U., Hugelius, G., Hocking, T. D., Lu, X., Shi, Z., Viatkin, K., Vargas, R., Yigini, Y., Omuto, C., Malik, A. A., Peralta, G., Cuevas-Corona, R., Di Paolo, L. E., Luotto, I., Liao, C., Liang, Y.-S., Saynes, V. S., Huang, X., and Luo, Y.: Microbial carbon use efficiency promotes global soil carbon storage, Nature, 618, 981–985, https://doi.org/10.1038/s41586-023-06042-3, 2023.

Tempest, D. W. and Neijssel, O. M.: Physiological and energetic aspects of bacterial metabolite overproduction, FEMS Microbiol. Lett., 100, 169–176, https://doi.org/10.1016/0378-1097(92)90205-3, 1992.

Thomas, M. R. and O'Shea, E. K.: An intracellular phosphate buffer filters transient fluctuations in extracellular phosphate levels, Proc. Natl. Acad. Sci. U. S. A., 102, 9565–9570, https://doi.org/10.1073/pnas.0501122102, 2005.

https://doi.org/10.5194/egusphere-2026-3590
Preprint. Discussion started: 30 June 2026

Veitia, R. A.: A sigmoidal transcriptional response: cooperativity, synergy and dosage effects, Biol. Rev. Camb. Philos. Soc., 78, 149–170, https://doi.org/10.1017/s1464793102006036, 2003.

Wang, B. and Allison, S. D.: Drought legacies mediated by trait trade-offs in soil microbiomes, Ecosphere, 12, https://doi.org/10.1002/ecs2.3562, 2021.

Wang, B. and Allison, S. D.: Climate-driven legacies in simulated microbial communities alter litter decomposition rates, Front. Ecol. Evol., 10, https://doi.org/10.3389/fevo.2022.841824, 2022.

Wanner, B. L.: Gene regulation by phosphate in enteric bacteria, J. Cell. Biochem., 51, 47–54, https://doi.org/10.1002/jcb.240510110, 1993.

Wieder, W. R., Bonan, G. B., and Allison, S. D.: Global soil carbon projections are improved by modelling microbial processes, Nat. Clim. Chang., 3, 909–912, https://doi.org/10.1038/nclimate1951, 2013.

Wutzler, T., Zaehle, S., Schrumpf, M., Ahrens, B., and Reichstein, M.: Adaptation of microbial resource allocation affects modelled long term soil organic matter and nutrient cycling, Soil Biol. Biochem., 115, 322–336, https://doi.org/10.1016/j.soilbio.2017.08.031, 2017.